Bioorganic Chemistry 67 (2016) 9–17

Contents lists available at ScienceDirect

Bioorganic Chemistry

journal homepage: www.elsevier.com/locate/bioorg

Identification of novel acetylcholinesterase inhibitors: Indolopyrazoline derivatives and molecular docking studies

Sridevi Chigurupati [a,*], Manikandan Selvaraj [b,c,*], Vasudevan Mani [c,d], Kesavanarayanan Krishnan Selvarajan [c], Jahidul Islam Mohammad [e], Balaji Kaveti [a], Hriday Bera [f], Vasanth Raj Palanimuthu [f], Lay Kek Teh [b,c], Mohd Zaki Salleh [b,c]

[a] Department of Pharmaceutical Chemistry, Faculty of Pharmacy, AIMST University, Semeling, 08100 Bedong, Kedah, Malaysia
[b] Integrative Pharmacogenomics Institute (iPROMISE), Universiti Teknologi MARA (UiTM), Puncak Alam Campus, 42300 Bandar Puncak Alam, Selangor Darul Ehsan, Malaysia
[c] Faculty of Pharmacy, Universiti Teknologi MARA (UiTM), Puncak Alam Campus, 42300 Bandar Puncak Alam, Selangor Darul Ehsan, Malaysia
[d] Department of Pharmacology and Toxicology, College of Pharmacy, Qassim University, Buraidah 51452, Saudi Arabia
[e] Department of Pharmacology, Faculty of Medicine, AIMST University, Semeling, 08100 Bedong, Kedah, Malaysia
[f] Department of Pharmaceutics, Faculty of Pharmacy, AIMST University, Semeling, 08100 Bedong, Kedah, Malaysia

ARTICLE INFO

Article history:
Received 7 April 2016
Revised 10 May 2016
Accepted 12 May 2016
Available online 13 May 2016

Keywords:
Indole
Pyrazoline
Molecular docking
Antioxidant
Acetylcholinesterase

ABSTRACT

The synthesis of novel indolopyrazoline derivatives (**P1-P4** and **Q1-Q4**) has been characterized and evaluated as potential anti-Alzheimer agents through *in vitro* Acetylcholinesterase (AChE) inhibition and radical scavenging activity (antioxidant) studies. Specifically, **Q3** shows AChE inhibition (IC_{50}: 0.68 ± 0.13 μM) with strong DPPH and ABTS radical scavenging activity (IC_{50}: 13.77 ± 0.25 μM and IC_{50}: 12.59 ± 0.21 μM), respectively. While **P3** exhibited as the second most potent compound with AChE inhibition (IC_{50}: 0.74 ± 0.09 μM) and with DPPH and ABTS radical scavenging activity (IC_{50}: 13.52 ± 0.62 μM and IC_{50}: 13.13 ± 0.85 μM), respectively. Finally, molecular docking studies provided prospective evidence to identify key interactions between the active inhibitors and the AChE that furthermore led us to the identification of plausible binding mode of novel indolopyrazoline derivatives. Additionally, *in-silico* ADME prediction using QikProp shows that these derivatives fulfilled all the properties of CNS acting drugs. This study confirms the first time reporting of indolopyrazoline derivatives as potential anti-Alzheimer agents.

1. Introduction

Cholinergic dysfunction and increased oxidative stress play an important role in the pathogenesis of Alzheimer's disease (AD). Acetylcholinesterase (AChE) is an enzyme that is responsible for the termination of cholinergic signalling by hydrolyzing acetylcholine (ACh). Therefore, inhibition of both AChE and oxidative stress could be effective in the treatment and management of AD [1]. Until recently, reversible AChE inhibitors (e.g. Donepezil, Rivastigmine and Galantamine) were used to treat the symptoms caused by cholinergic dysfunction in AD [2]. However, the related enzyme butyrylcholinesterase also hydrolyses Ach but, AChE inhibitors are commonly prescribed to improve the cholinergic signalling in AD. The use of the above class of drugs for the treatment of AD has been limited by its serious side effects, so the search for novel compounds remains as an emerging demand for the treatment of AD. Indole alkaloids and its analogues are well known for their AChE inhibitory [3–5] and antioxidant effects [5–7]. Pyrazolines are also well known for various biological activities including antioxidant [8] and cholinesterase and selective monoamine oxidase B inhibitors for the treatment of AD [9,10] and Parkinson's disease [11]. There are various report which showed that the hybrid of two active moiety enhance the activity like hybrids of indole, quinoline, bisindole, benzothiazole, benzimidazole, biscoumarin, oxadiazole showed potent activity [12–18].

Both pyrazoline and indole nucleus are potent AChE inhibitors. Till date, no studies are reported in hybrid of these two nuclei and investigated either as an AChE inhibitor or antioxidant.

In the present study, the 3-acetylindole moiety is modified into indolopyrazolines (**P1-P4** and **Q1-Q4**) *via* indolochalcones as

* Corresponding authors at: Integrative Pharmacogenomics Institute (iPROMISE), Universiti Teknologi MARA (UiTM), Puncak Alam Campus, 42300 Bandar Puncak Alam, Selangor Darul Ehsan, Malaysia. Tel.: +60 33258 4652; fax: +60 33258 4658 (S. Manikandan), Department of Pharmaceutical Chemistry, Faculty of Pharmacy, AIMST University, Semeling 08100, Bedong, Kedah, Malaysia. Tel.: +60 4429 8000x1284 (Ch. Sridevi).

E-mail addresses: sridevi.phd@gmail.com (S. Chigurupati), manifans@gmail.com (M. Selvaraj).

http://dx.doi.org/10.1016/j.bioorg.2016.05.002
0045-2068/

intermediate compounds. The synthesized compounds were characterized and evaluated for their possible *in vitro* antioxidant and AChE inhibitory potentials.

Each experimental value is expressed as the mean ± Standard error mean and all experiments are carried in triplicates (n = 3). Statistical analysis was performed using Graph Pad prism 5.0.

Molecular docking studies were carried out [15] further to explore the feasibility of the structural topographies required for the interaction of the indolopyrazoline derivatives with the AChE enzyme. It also permits to elucidate the possible key active site residues involved in the intermolecular interactions with the ligand [19]. So furthermore, the synthesized compounds were evaluated for their possible QikProp prediction of ADME properties for all the eight indolopyrazoline derivatives [20].

2. Results and discussion

2.1. Chemistry

Indolopyrazolines (**P1-P4** and **Q1-Q4**) were obtained by refluxing the indolochalcones (**III** and **V**) and acid hydrazides in 1:2 ratio respectively in the presence of glacial acetic acid (see Schemes 1 and 2). The mechanism involved in the conversion of chalcone to pyrazole is given in Fig. 1 The indolochalcones were obtained by Aldol condensation of 3-acetyl indole and substituted benzaldehydes in the presence of aqueous NaOH Solution. Solidified crude products were recrystallized from aqueous ethanol. The indolopyrazolines were obtained in high yields. The purity of the indolopyrazoline compounds was checked by the R_f value of TLC (Thin Layer

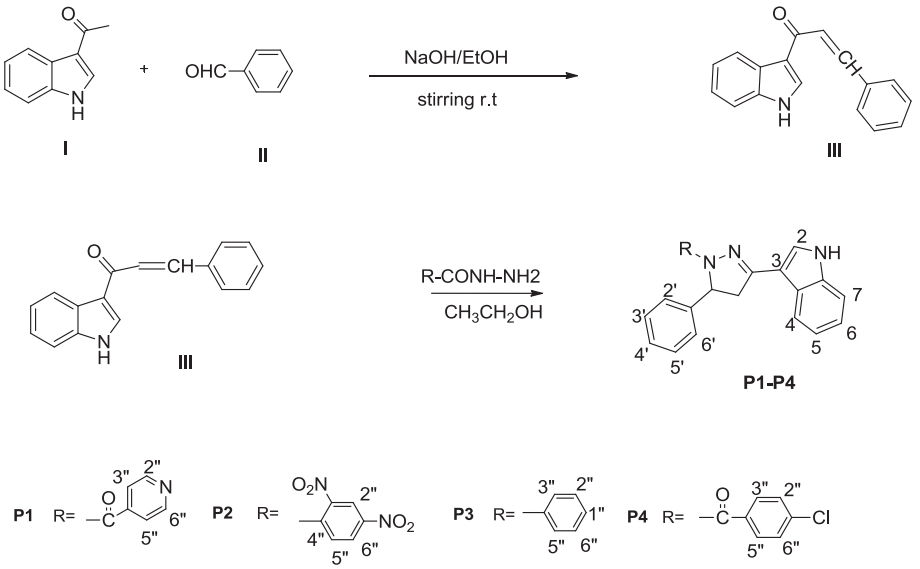

Scheme 1. Synthesis of indolopyrazolines (**P1-P4**).

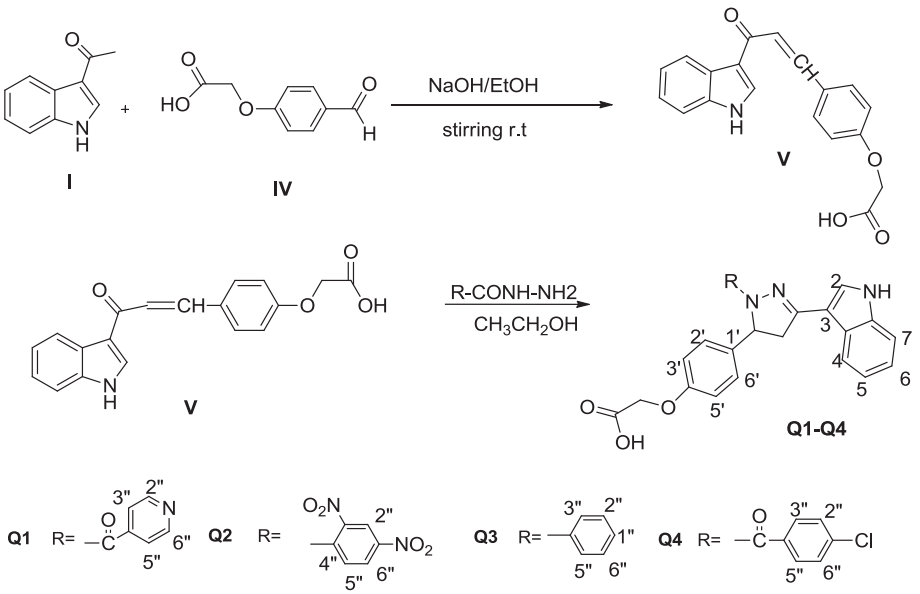

Scheme 2. Synthesis of indolopyrazolines (**Q1-Q4**).

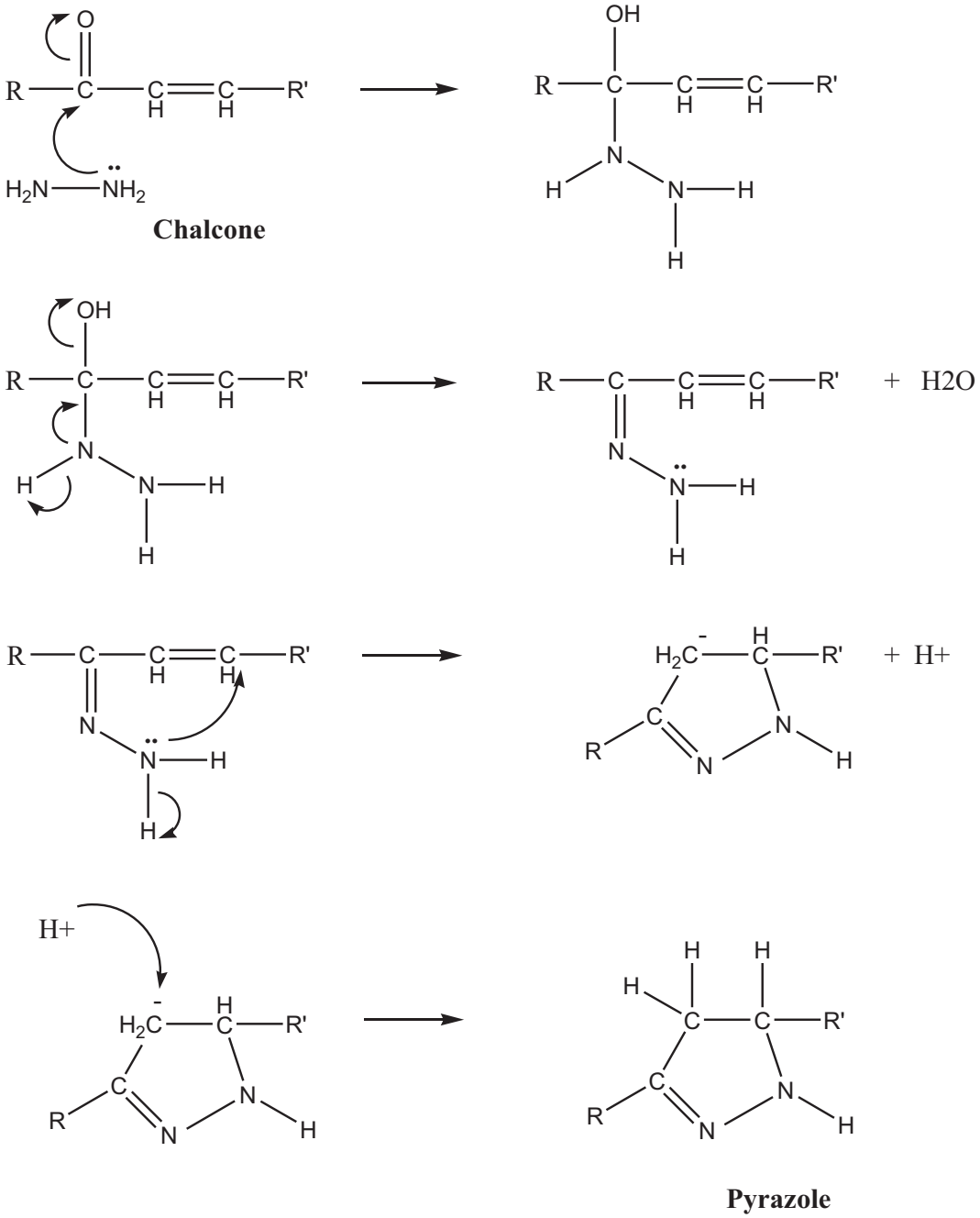

Fig. 1. The mechanism involved in the conversion of chalcone to pyrazole.

Chromatography) and melting point. Physical data and spectroscopic techniques like UV–Visible, ^{1}H NMR, mass spectra and CHN analysis confirmed the structures and purity of the synthetic compounds.

The λ_{max} for the newly synthesized indolopyrazolines was found to be in the range of 300–440 nm. The formation of pyrazoline was revealed by the presence of doublet between 2.12–2.16 ppm and a triplet at 4.51–4.58 ppm in proton NMR spectra. All other aliphatic and aromatic protons were observed within the expected regions. The compounds were further confirmed by their characteristic mass fragment spectra. The mass fragment pattern of compound **P4** given in Fig. 2, displayed parent ion peak at 399, base peak at 51, and different fragment peaks at 139, 117, 42 and 20. Similarly, all the novel compounds were characterized. This part confirmed the synthesis of a series of eight new indolopyrazoline compounds.

2.2. Antioxidant assay

The *in vitro* antioxidant potential of synthesized indolopyrazolines (**P1-P4** and **Q1-Q4**) was evaluated using DPPH (1,1-Diphenyl-2-picrylhydrazyl) stable free radical, ABTS (2,2′-azinobis (3-ethyl benzothiazoline-6-sulfonic acid) radical cation scavenging assay and compared to ascorbic acid. The results revealed that all the indolopyrazolines are good at scavenging free radicals of DPPH and ABTS when compared with the reference standard, ascorbic acid at the same concentrations. However, on finding the IC_{50}

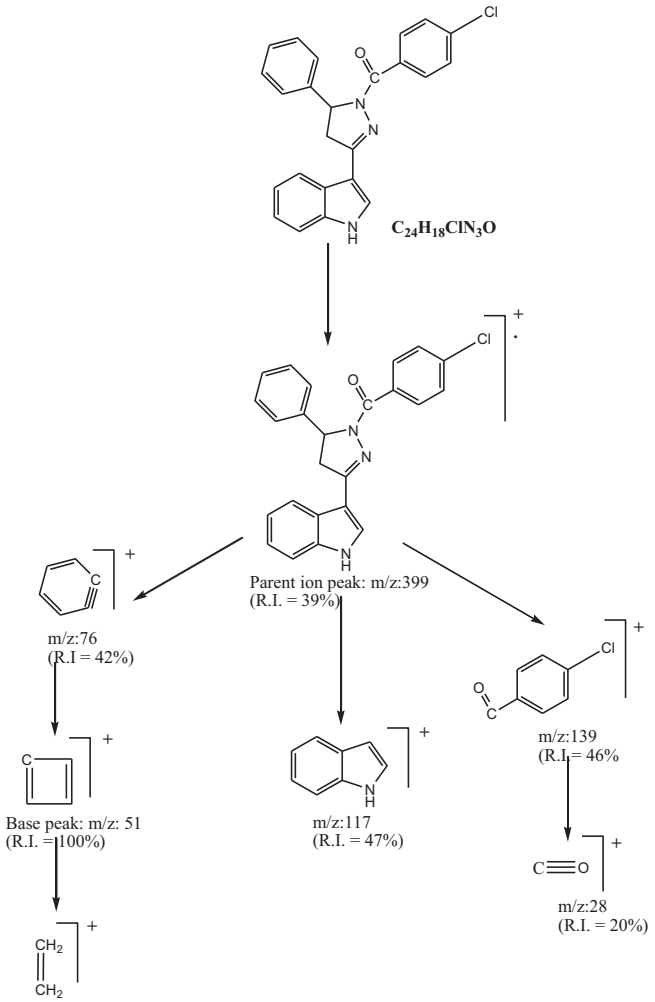

Fig. 2. Mass fragmentation pattern of **P4**.

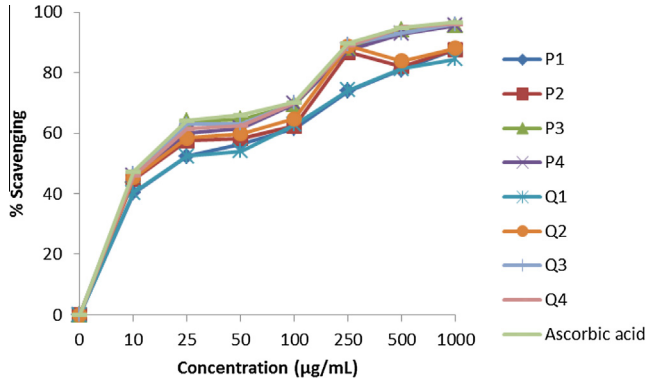

Fig. 3. DPPH radical scavenging assay results of indolopyrazolines.

values of eight compounds, **P3** and **Q3** were proved to be the best compounds in scavenging free radicals (see Figs. 3 and 4).

In DPPH assay, the IC_{50} values obtained with the compounds (**P1-P4**; **Q1-Q4**) showed varying degree of activities in terms of the IC_{50} value (see Table 1). The IC_{50} values obtained with three compounds, namely, **P3** (13.52 ± 6.2), **Q3** (13.77 ± 2.5) and **Q4** (14.86 ± 2.4) were comparable with that of the positive control, ascorbic acid (12.79 ± 1.9). Similarly, in ABTS assay, these compounds also showed better IC_{50} values with compounds **Q3**

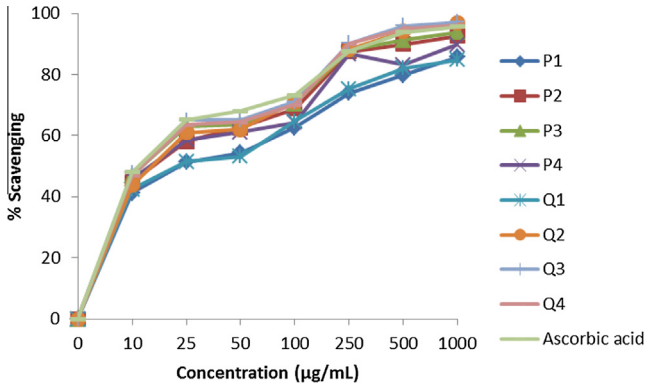

Fig. 4. ABTS radical cation scavenging assay results of indolopyrazolines.

(12.59 ± 6.1), **P3** (13.13 ± 2.5) and **Q4** (13.38 ± 0.33) and the IC_{50} values were also comparable to ascorbic acid (11.5 ± 1.9).

2.3. Anticholinesterase enzyme inhibition assay

In AChE assay, compounds **Q3** (0.68 ± 0.13) and **P3** (0.74 ± 0.09) showed better IC_{50} values compared to that of the positive control, Donepezil (0.01 ± 0.4). It is notable that out of the eight synthesized compounds, **P3** and **Q3** performed well in both AChE and antioxidant assays.

2.4. Docking studies and binding mode analysis

Molecular modeling studies were accomplished to investigate the possible binding mode of eight indolopyrazoline derivatives (**P1-P4** and **Q1-Q4**) targeting the crystal structure of acetyl cholinesterase (PDB ID: 1EVE) using Glide docking program, Schrodinger Maestro software (version 6.9; Schrodinger LLC, New York). All the eight indolopyrazoline derivatives were docked into the active site of the AChE. The results were analyzed based on the glide docked scores obtained from GLIDE (Grid-based Ligand Docking with Energetics) docking [21]. The docked binding mode was analyzed for the interactions between specific compounds and AChE. In-depth analysis of the interaction pattern for the most active compounds **P3, P4, Q3** and **Q4** are detailed in the following section. The binding mode of the compound **P3** positioned in the ravine of the AChE active site showed that Phe288 of the AChE form hydrogen bond with oxygen attached to the methanone group. The two phenyl groups of the **P3** form π-π stacking with Trp279, while the residues such as Trp84, Phe330, Tyr121, Ile287, Tyr334 and Phe331 forms hydrophobic interaction with an indole and pyrazol ring of compound **P3** as shown in Fig. 5a.

Fig. 5b shows the docking orientation of compound **P4,** where the Phe288 of the AChE forms hydrogen bond with methanone oxygen, while the phenyl group forms hydrophobic interactions with Phe290, Tyr334 and Tyr121 while a chlorophenyl ring of the **P4** forms hydrophobic interaction with Ile287. Additionally, the indole ring forms hydrophobic contact with Trp84, Phe330 and Phe331.

The compound **Q3** as shown in Fig. 6a quartered in the active site of AChE form stable network of hydrogen bonding between the indole NH with His440 and the acetic acid oxygens forming hydrogen bonds with Arg289 and Phe288, respectively. Specifically, the indole ring also forms stable π-π stacking with Trp84 and His440, respectively.

The complex is also stabilized by the hydrophobic interaction established between the benzene ring of **Q3** with Tyr70 and

Table 1
IC_{50} values of indolopyrazolines.

Compound code	Chemical structure	IC_{50} (μM ± SEM[a])		
		DPPH radical scavenging assay	ABTS radical cation scavenging assay	AChE inhibition assay
P1	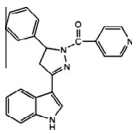	25.18 ± 0.94	25.52 ± 0.64	10.58 ± 0.34
P2	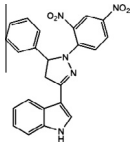	17.43 ± 0.44	16.12 ± 0.73	60.82 ± 0.15
P3	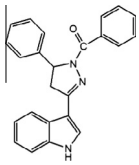	13.52 ± 0.62	13.13 ± 0.85	0.74 ± 0.09
P4	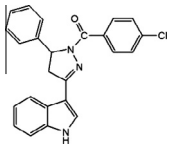	15.42 ± 0.98	15.48 ± 1.11	9.72 ± 0.29
Q1	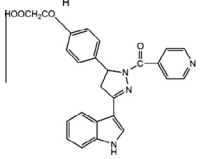	25.45 ± 1.4	24.25 ± 0.9	86.56 ± 0.97
Q2	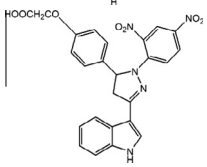	15.99 ± 0.92	16.16 ± 0.34	27.13 ± 0.31
Q3	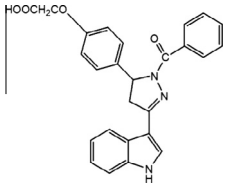	13.77 ± 0.25	12.59 ± 0.21	0.68 ± 0.13
Q4	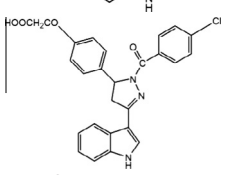	14.86 ± 0.14	13.38 ± 0.13	8.67 ± 0.33
Ascorbic acid	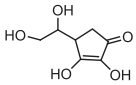	12.79 ± 0.99	11.5 ± 0.89	–
Donepezil	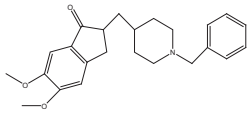	–	–	0.01 ± 0.40

[a] Standard mean error using Graph Pad prism 5 (n = 3).

Tyr121. Additionally, pyrazole phenoxy ring forms hydrophobic interactions with Ile287, Tyr334, Phe331 and Phe330.

In the case of **Q4** the orientation of ligands forms a stable network of hydrogen bonding between the indole NH with His440 and the acetic acid oxygen's forming hydrogen bonds with Arg289 and Phe288, respectively. In addition, the indole ring also forms stable π-π stacking with Trp84, His440 and hydrophobic interactions with Phe330 and Tyr130. Moreover, the chlorobenzene ring forms hydrophobic interactions with Tyr121, Tyr70, Val71 and Pro86. Likewise, the phenoxy group also forms hydrophobic interactions with Ile287, Tyr334 and Phe331 (Fig. 6b).

AChE inhibitory activities for compound **Q1**-**Q4** varies due to the presence of different substituted aryl groups at 'R' position. Existence of electron withdrawing groups in the aryl group

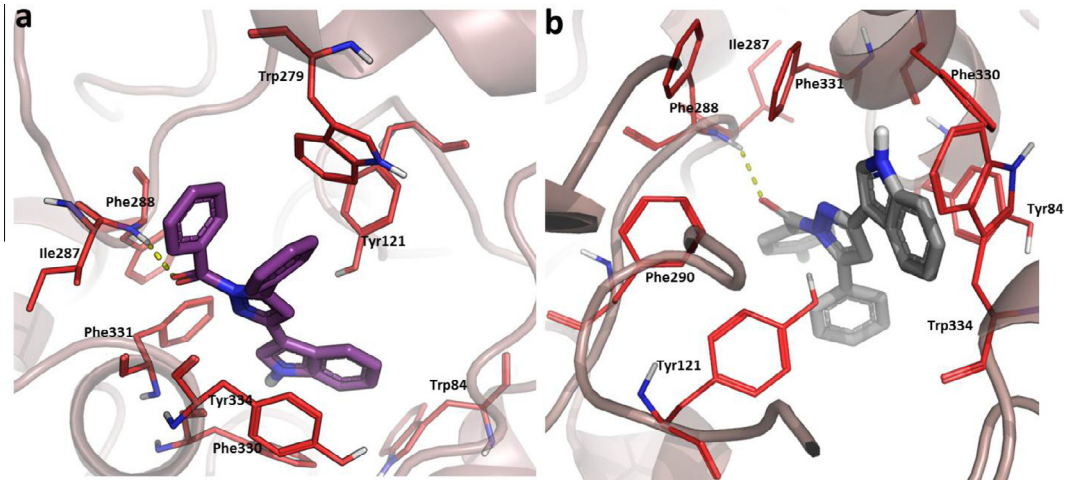

Fig. 5. Shows the binding mode of the compound in stick (a) compound **P3** and (b) compound **P4** in the AChE active site. Key interacting residues are shown in line, and the hydrogen bonds are represented by a yellow dashed line.

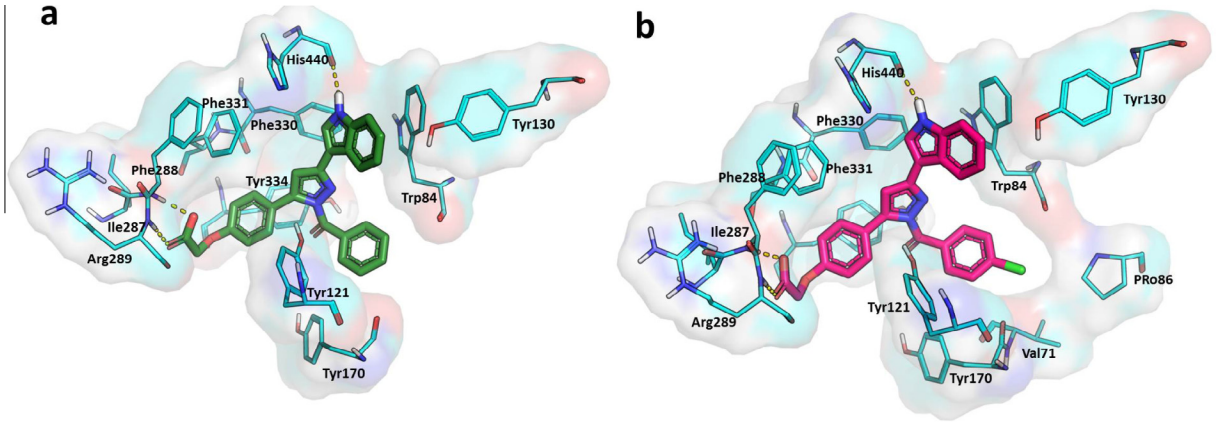

Fig. 6. Shows the binding mode of the compound in stick (a) compound **Q3** and (b) compound **Q4** in the AChE active site. Key interacting residues are shown in line, and the hydrogen bonds are represented as a dashed yellow line.

decreases the activity. Through docking studies it's evident that the existence of AChE hydrophobic residues at the site of 'R' group interacting site (aryl group) does not prefer electron withdrawing groups, which eventually decrease the activity. Hence the activity profile of compound **Q1**-**Q4** varies. In the case of compound **Q4** the presence of Cl has the tendency to donate electron, so its activity is better compared to nitro group (compound **Q2**) and pyridine (compound **Q1**) which are electron withdrawing groups. In turn compound **Q3** with a simple aryl group such as benzene without any electron withdrawing group ranks top in the activity profile, thus establishing possible hydrophobic interactions with the active site hydrophobic residues of AChE.

2.5. Theoretical ADME prediction of indolopyrazoline derivatives

Theoretical calculations of the ADME (Absorption, Distribution, Metabolism and Excretion) properties of indolopyrazoline derivatives (**P1**-**P4** and **Q1**-**Q4**) were done using QikProp [20]. Drug kinetics and exposure of tissues to drug influences the pharmacological activity and the performance of a drug, which is ultimately determined by its ADME properties. Nearly 12 physically significant descriptors and pharmacologically relevant properties of indolopyrazoline derivatives were predicted and analyzed (Supplementary Material, Table S1).

Aqueous solubility (QPlogS) of organic compounds plays a key impact on many ADME associated properties like uptake, distribution, transport, and ultimately bioavailability. Eight of our indolopyrazoline derivatives solubility values were within the range [22]. Further, the predicted values for the blood–brain barrier (BBB) penetration of all the compounds seems to be in the optimum penetrate range (−2 to +2 scale) and consequently are measured as active compounds on the CNS. Finally, the Lipinski's rule of five and Qikprop rule of three were all within the range for the indolopyrazoline derivatives and thus making these derivatives as suitable drug candidates.

3. Conclusions

In conclusion, eight indolopyrazoline derivatives were synthesized and assessed for AChE inhibition and antioxidant activity agents against AD. The biological activity assay confirms that most of the indolopyrazoline derivatives were potent inhibitors of AChE. Particularly compound **Q3** possessing phenyl moiety was found to be the best potent AChE inhibitor (IC_{50}: 0.68 ± 0.13 μM) with strong DPPH and ABTS radical scavenging activity with IC_{50}: 13.77 ± 0.25 μM and IC_{50}: 12.59 ± 0.21 μM, respectively. While compound **P3** exhibited as the second most potent compound (IC_{50}: 0.74 ± 0.09 μM) with DPPH and ABTS radical scavenging activity IC_{50}: 13.52 ± 0.62 μM and IC_{50}:13.13 ± 0.85 μM, respectively. In this case, **Q3** and **P3** are the most potent compounds bearing phenyl moiety among all the indolopyrazoline derivatives. Besides, the above mentioned potent compounds, **Q4** and **P4** are

the second level compounds in the activity profile as shown in Table 1. Interestingly, both **Q4** and **P4** bears chlorophenyl moiety that establishes an interaction with the hydrophobic residue in the active site of AChE.

Docking studies and the inhibition assay revealed the capability of indolopyrazoline derivatives to bind the AChE and induces strong inhibitory effect. Qikprop prediction of ADME properties indicates that compounds are CNS active and fulfilled the Lipinski's rule of five. Collectively, the results propose that the indolopyrazoline derivatives, specifically compound **Q3, P3, Q4** and **P4** could be deliberated as the potential drug candidates for AD.

4. Experimental

4.1. General

All the solvents and chemicals used were of analytical grade and obtained from Sigma-Aldrich and Merck Pvt. Ltd., and were used without further purification. The melting points of the compounds were determined on a Thoshniwal electric melting point apparatus and the values were uncorrected. The purity of all the compounds was routinely checked by TLC on Silica gel-GF 254 (Merck) coated plates. Spots of TLC were identified by iodine chamber. The UV–Visible spectra of the compounds were recorded on double beam Shimadzu UV1800 spectrophotometer. ^{1}H NMR spectra were recorded on Bruker UX-NMR Instrument, using TMS as an internal standard, $CDCl_3$ as solvent; and chemical shift values were expressed in δ ppm. Elemental analyses of synthesized compounds were done over Perkin Elmer 240 CHN Analyzer.

4.2. General procedure for synthesis of indolochalcones (*III* and *V*)

Aldol condensation was carried out by the following method, a solution of NaOH (8 mL, 10% in water) was added drop wise to a well stirred solution of 0.01 M of 3-acetyl indole and 0.01 M of benzaldehyde and p-formyl phenoxy acetic acid respectively, in 20 mL ethanol at cold temperature [23,24]. The reaction mixture was then stirred for 24 h in ice bath. The reaction was monitored by TLC. The mixture was then diluted with ice water and acidified with concentrated HCl. The product was filtered and dried. The product was recrystallized with aqueous ethanol. The purity of the compound was checked by the Rf value of TLC and melting point.

4.3. General procedure for synthesis of indolopyrazolines (*P1-P4* and *Q1-Q4*)

0.01 M of chalcone and 0.02 M of four different benzoic acid hydrazides (isonicotino hydrazide, 2,4 dinitrophenyl hydrazine, benzohydrazide, 4-chlorobenzohydrazide) were taken with 20 mL glacial acetic acid and refluxed for 10 h above 130 °C separately. The reaction mixtures were then concentrated and poured into 300 mL of ice-cold water [25,26]. The formed products were filtered and dried. The products were recrystallized with aqueous ethanol (see Schemes 1 and 2). The purity of the indolopyrazoline compounds was checked by the R_f value of TLC and melting point. The structures of indolopyrazolines (**P1-P4** and **Q1-Q4**) were characterized by spectral data.

4.3.1. (3-(1H-indol-3-yl)-5-phenyl-4,5-dihydropyrazol-1-yl) (pyridin-4-yl) methanone (*P1*)

Yield: 86%, mp: 170–172 °C, R_f (TLC): 0.57, ^{1}H NMR (500.1 MHz, $CDCl_3$-*d*): δ/ppm 2.12 (2H, d, *J* = 7, CH_2 of pyrazoline), 4.56 (1H, t, *J* = 7, CH of pyrazoline), 6.23 (1H, d, *J* = 7.2 Hz, =CH of indole), 6.84–7.06 (5H, m, Ar-H2′, H3′, H4′, H5′, H6′) 7.12–7.45 (4H, m, Ar-H4, H5, H6, and H7), 8.01 (2H, d, *J* = 8.5 Hz, Ar-H3″, H5″), 9.04 (2H, d, *J* = 8.5 Hz, Ar-H2″, H6″), 9.53 (1H, brs, NH group of indole ring); Anal. Calcd for $C_{23}H_{18}N_4O$: C = 75.39, H = 4.95, N = 15.29. Found: C = 75.29, H = 4.94, N = 15.27; MS (*m/z*, (relative abundance, %)): 366 (M^+), 116, 106, 78, 76, 51, 28, 27, 26; UV–vis (MeOH) (λ_{max}/nm): 295.

4.3.2. (3-(1H-indol-3-yl)-5-phenyl-4,5-dihydropyrazol-1-yl) (2,4dinitrophenyl) methanone (*P2*)

Yield: 86%, mp: 200–202 °C, R_f (TLC): 0.62, ^{1}H NMR (500.1 MHz, $CDCl_3$-*d*): δ/ppm 2.16 (2H, d, *J* = 7.0 Hz, CH_2 of pyrazoline), 4.54 (1H, t, *J* = 7.0 Hz, CH of pyrazoline), 6.22 (1H, d, *J* = 7.2 Hz, =CH of indole), 6.85–7.07 (5H, m, Ar-H2′, H3′, H4′, H5′, H6′), 7.16–7.48 (4H, m, Ar-H4, H5, H6, and H7), 8.56–9.25 (3H, m, Ar-H2″, H5″, H6″), 9.54 (1H, brs, NH group of indole ring); Anal. Calcd for $C_{23}H_{17}N_5O_4$: C = 64.03, H = 4.01, N = 16.39. Found: C = 64.01, H = 4.00, N = 16.37; MS (*m/z*, (relative abundance, %)): 427 (M^+), 167, 116, 76, 51, 46, 30, 27, 26; UV–vis (MeOH) (λ_{max}/nm): 333.

4.3.3. (3-(1H-indol-3-yl)-5-phenyl-4,5-dihydropyrazol-1-yl) (phenyl) methanone (*P3*):

Yield: 86%, mp: 142–144 °C, R_f (TLC): 0.58, ^{1}H NMR (500.1 MHz, $CDCl_3$-*d*): δ/ppm 2.14 (2H, d, *J* = 7.0 Hz, CH_2 of pyrazoline), 4.52 (1H, t, *J* = 7.0 Hz, CH of pyrazoline), 6.24 (1H, d, *J* = 7.2 Hz, =CH of indole), 6.83–7.04 (5H, m, Ar-H2′, H3′, H4′, H5′, H6′), 7.15–7.46 (4H, m, Ar-H4, H5, H6, and H7), 7.7–8.01 (6H, m, Ar-H2″, H3″, H4″, H5″, H6″), 9.51 (1H, brs, NH group of indole ring); Anal. Calcd for $C_{24}H_{19}N_3O$: C = 78.88, H = 5.24, N = 11.50. Found: C = 78.84, H = 5.22, N = 11.51; MS (*m/z*, (relative abundance, %)): 365 (M^+), 116, 111, 76, 51, 28, 27, 26; UV–vis (MeOH) (λ_{max}/nm): 312.

4.3.4. (3-(1H-indol-3-yl)-5-phenyl-4,5-dihydropyrazol-1-yl) (4-chlorophenyl) methanone (*P4*)

Yield: 86%, mp: 156–158 °C, R_f (TLC): 0.65, ^{1}H NMR (500.1 MHz, $CDCl_3$-*d*): δ/ppm 2.14 (2H, d, *J* = 7.0 Hz, CH_2 of pyrazoline), 4.54 (1H, t, *J* = 7, CH of pyrazoline), 6.22 (1H, d, *J* = 7.2 Hz, =CH of indole), 6.87–7.08 (5H, m, Ar-H2′, H3′, H4′, H5′, H6′), 7.12–7.44 (4H, m, Ar-H4, H5, H6 and H7), 7.62 (2H, d, *J* = 8.5 Hz, Ar-H2″, H6″), 7.91 (2H, d, *J* = 8.5 Hz, Ar-H3″, H5″), 9.51 (1H, brs, NH group of indole ring); Anal. Calcd for $C_{24}H_{18}ClN_3O$: C = 72.09, H = 4.54, N = 10.51. Found: C = 72.11, H = 4.56, N = 10.54; MS (*m/z*, (relative abundance, %)): 399 (M^+), 116, 76, 51, 36, 28, 27, 26; UV–vis (MeOH) (λ_{max}/nm): 325.

4.3.5. 2-(4-(3-(1H-indol-3-yl)-1-isonicotinoyl-4,5-dihydro-1H-pyrazol-5-yl) phenoxy) acetic acid (*Q1*)

Yield: 68%, mp: 152–154 °C, R_f (TLC): 0.54, ^{1}H NMR (500.1 MHz, $CDCl_3$-*d*): δ/ppm 2.14 (2H, d, *J* = 7.0 Hz, CH_2 of pyrazoline), 4.54 (1H, t, *J* = 7.0 Hz, CH of pyrazoline), 4.89 (2H, s, OCH_2), 6.21 (1H, d, *J* = 7.2 Hz, =CH of indole), 6.65 (2H, d, *J* = 8.4 Hz, Ar-H3′, H5), 6.98 (2H, d, *J* = 8.4 Hz, Ar-H2′, H6), 7.14–7.48 (4H, m, Ar-H4, H5, H6, and H7), 7.91 (2H, d, *J* = 8.5 Hz, Ar-H3″, H5″), 9.04 (2H, d, *J* = 8.5 Hz, Ar-H2″, H6″), 9.51 (1H, brs, NH group of indole ring), 11.25 (1H, brs, OH carboxylic acid group); Anal. Calcd for $C_{25}H_{22}N_4O_4$: C = 67.86, H = 5.01, N = 12.66. Found: C = 67.84, H = 5.03, N = 12.64; MS (*m/z*, (relative abundance, %)): 442 (M+), 151, 116, 76, 51, 44, 42, 43, 28, 26, 18, 27; UV–vis (MeOH) (λ_{max}/nm): 320.

4.3.6. 2-(4-(1-(2,4-dinitrobenzoyl)-3-(1H-indol-3-yl)-4,5-dihydro-1H-pyrazol-5-yl) phenoxy) acetic acid (*Q2*)

Yield: 78%, mp: 152–154 °C, R_f (TLC): 0.76, ^{1}H NMR (500.1 MHz, $CDCl_3$-*d*): δ/ppm 2.12 (2H, d, *J* = 7.0 Hz, CH_2 of pyrazoline), 4.58 (1H, t, *J* = 7.0 Hz, C—H of pyrazoline), 4.82 (2H, s, OCH2), 6.22 (1H, d, *J* = 7.2 Hz, =C—H of indole), 6.63 (2H, d, *J* = 8.4 Hz, Ar-H3′, H5′), 6.94 (2H, d, *J* = 8.4 Hz, Ar-H2′, H6′), 7.32–7.59 (4H, m,

Ar-H4, H5, H6, and H7), 7.96 (2H, d, *J* = 8.5, Ar-H3″, H5″), 8.98 (2H, d, *J* = 8.5 Hz, Ar-H2″, H6″), 9.51 (1H, brs, NH group of indole ring), 11.24 (1H, brs, OH carboxylic acid group); Anal. Calcd for $C_{25}H_{22}N_4O_4$: C = 59.64, H = 4.20, N = 13.91. Found: C = 59.62, H = 4.19, N = 13.89; MS (*m/z*, (relative abundance, %)): 503 (M+), 151, 116, 76, 51, 46, 44, 42, 43, 30, 26, 27, 18; UV–vis (MeOH) (λ_{max}/nm): 302.

4.3.7. 2-(4-(1-benzoyl-3-(1H-indol-3-yl)-4,5-dihydro-1H-pyrazol-5-yl) phenoxy) acetic acid ***(Q3)***

Yield: 58%, mp: 142–144 °C, R_f (TLC): 0.63, ^{1}H NMR (500 MHz, $CDCl_3$-*d*): δ/ppm 2.15 (2H, d, *J* = 7.0 Hz, CH2 of pyrazoline), 4.55 (1H, t, *J* = 7.0 Hz, C—H of pyrazoline), 4.82 (2H, s, OCH_2), 6.23 (1H, d, *J* = 7.2 Hz, =C—H of indole), 6.62 (2H, d, *J* = 8.4 Hz, Ar-H3′, H5′), 6.95 (2H, d, *J* = 8.4 Hz, Ar-H2′, H6′), 7.32–7.59 (4H, m, Ar-H4, H5, H6, and H7), 7.62–7.96 (5H, m, Ar-H2″, H3″, H4″, H5″, H6″), 9.54 (1H, brs, NH group of indole ring), 11.21 (1H, brs, OH carboxylic acid group); Anal. Calcd for $C_{26}H_{23}N_3O_4$: C = 70.73, H = 5.25, N = 9.52. Found: C = 70.70, H = 5.23, N = 9.50; MS (*m/z*, (relative abundance, %)): 441 (M+), 151, 116, 76, 51, 44, 42, 43, 30, 28, 26, 27, 18, 51; UV–vis (MeOH) (λ_{max}/nm): 359.

4.3.8. 2-(4-(1-(4-chlorobenzoyl)-3-(1H-indol-3-yl)-4,5-dihydro-1H-pyrazol-5-yl) phenoxy) acetic acid ***(Q4)***

Yield: 72%, mp: 122–124 °C, R_f (TLC): 0.59, ^{1}H NMR (500.1 MHz, $CDCl_3$-*d*): δ/ppm 2.12 (2H, d, *J* = 7.0 Hz, CH_2 of pyrazoline), 4.51 (1H, t, *J* = 7.0 Hz, C—H of pyrazoline), 4.87 (2H, s, OCH_2), 6.27 (1H, d, *J* = 7.2 Hz, =C—H of indole), 6.69 (2H, d, *J* = 8.4 Hz, Ar-H3′, H5′), 6.98 (2H, d, *J* = 8.4 Hz, Ar-H2′, H6′), 7.32–7.58 (4H, m, Ar-H4, H5, H6, and H7), 7.84 (2H, d, *J* = 8.5, Ar-H2″, H6″), 7.98 (2H, d, *J* = 8.5 Hz, Ar-H3″, H5″), 9.54 (1H, brs, NH group of indole ring), 11.24 (1H, brs, OH carboxylic acid group); Anal. Calcd for $C_{26}H_{22}ClN_3O_4$: C = 65.62, H = 4.66, N = 8.83. Found: C = 65.60, H = 4.63, N = 8.82; MS (*m/z*, (relative abundance, %)): 475 (M+), 151, 116, 76, 44, 42, 43, 30, 28, 26, 36, 27, 18, 51; UV–vis (MeOH) (λ_{max}/nm): 299.

4.4. DPPH radical scavenging assay

Preparation of DPPH solution was adopted from Molyneux [27] and Blois [28] with minor modification. All the test compounds were dissolved in 95% ethanol. Briefly, 0.5 mL of test compounds were added (0 - blank control, 10, 25, 50, 100, 250, 500 and 1000 μg/mL) to 0.5 mL of DPPH (2 μM in 95% ethanol) and the mixture was incubated at room temperature for 30 min. The absorbance was measured at 517 nm [8], and the percentage inhibition of test compounds was calculated using the following equation using Microsoft Excel software (version 2010). Ascorbic acid was used as the positive control [29].

$$\% \text{ Inhibition} = (1 - \text{absorbance sample}/\text{absorbance control}) \times 100 \quad (1)$$

The IC_{50} (half maximal inhibitory concentration) was calculated by constructing a non-linear regression graph between % inhibition *vs* concentration, using Graph Pad prism software (version 5).

4.5. ABTS free-radical cation scavenging assay

The ABTS free radical cation scavenging ability of the synthesized compounds was determined according to the procedure described earlier [30]. ABTS was dissolved in distilled water (7×10^{-3} M) and potassium persulphate (2.45×10^{-3} M) was added. This reaction mixture was left overnight (12–16 h) in the dark, at room temperature. Various concentrations of test substances (1000 μg/mL 500 μg/mL, 250 μg/mL, 100 μg/mL, 50 μg/mL, 25 μg/mL, 10 μg/mL concentrations) were incubated with the ABTS+· solution for 30 min. The absorbance was measured at 734 nm, and the % inhibition was calculated using the formula described in Eq. (1) and the IC_{50} was calculated. Ascorbic acid was used as the positive control.

4.6. Anticholinesterase enzyme inhibition assay

The *in vitro* AChE inhibitory activity was measured using the methods described earlier [31]. Briefly, stock solutions (1 mg/mL) of test compounds were prepared using DMSO. Working solutions (0.01–100 μg/mL) were prepared by serial dilutions. The various concentrations of test compounds (10 μL) were pre-incubated with sodium phosphate buffer (0.1 M; pH 8.0; 150 μL), and AChE solution (0.1 U/mL; 20 μL) for 15 min at 25 °C. The reaction was initiated by addition of DTNB (10 mM; 10 μL) and ATChI (14 mM; 10 μL). The reaction mixture was mixed using a cyclomixer and incubated for 10 min at room temperature. The absorbance was measured using a microplate reader at 410 nm wavelength against the blank reading containing 10 μL DMSO instead of test compound. The % inhibition was calculated using the formula described in Eq. (1) and the IC_{50} was calculated. Donepezil (0.01–100 μg/mL) was used as the positive control.

4.7. Molecular modeling, Docking and ADME study

In order to reveal the binding modes of our eight synthesized indolopyrazoline derivatives, docking simulation was performed targeting the crystal structure acetyl cholinesterase (PDB ID: 1EVE) [32]. Prior to docking, the crystal structure of the AChE enzyme was prepared using protein preparation wizard. The crystal structure was retrieved from the protein data bank (PDB), and the structure was optimized by removing the water molecules, hetero atoms and co-factors. Hydrogen, missing atoms, bonds and charges were computed through Maestro [33]. The eight synthesized indolopyrazoline derivatives used for docking were ligand prepared and optimized using built and LigPrep module implemented in Schrodinger Maestro. Ligands preparation includes generating various tautomers, assigning bond orders, ring conformations and stereo chemistries. All the conformations generated were minimized using OPLS2005 force field prior to docking study. Further, a receptor grid was generated around the AChE enzyme active site by choosing centroid of AChE enzyme complexed ligand (Aricept). Grid box size was set to 20 Å radius, using receptor grid generation implemented in Glide [33].

Docking calculations were accomplished using Glide: a complete solution for ligand-receptor docking implemented in small molecule drug discovery suite [33] and as well following the methods suggested by Taha et al. [15]. All docking calculations were performed using Standard Precision (SP) mode and Extra Precision (XP) mode. The Glide docking score was used to determine the best docked structure from the output. The interactions of these docked complexes were further analyzed and imaged using PyMOL [34]. Additional, Qikprop prediction of ADME properties were done for all the eight indolopyrazoline derivatives [20].

Acknowledgment

The authors are thankful to AIMST University, Malaysia for providing the facilities for this project and the Ministry of Higher Education, Malaysia (MOHE) for funding the computational part (Software and Workstation) through the "TRGS" (grant no. 600-RMI/TRGS 5/3 (1/2014)-3).

Appendix A. Supplementary material

Supplementary data associated with this article can be found, in the online version, at http://dx.doi.org/10.1016/j.bioorg.2016.05.002.

References

[1] M. Moniruzzaman, M. Asaduzzaman, M.S. Hossain, J. Sarker, S.M. Rahman, M. Rashid, M.M. Rahman, *In vitro* antioxidant and cholinesterase inhibitory activities of methanolic fruit extract of *Phyllanthus acidus*, BMC Complement. Altern. Med. 15 (2015) 403.

[2] R.M. Lane, M. Kivipelto, N.H. Greig, Acetylcholinesterase and its inhibition in Alzheimer disease, Clin. Neuropharmacol. 27 (3) (2004) 141–149.

[3] M. Khoobi, F. Ghanoni, H. Nadri, A. Moradi, M. Pirali Hamedani, F. Homayouni Moghadam, S. Emami, M. Vosooghi, R. Zadmard, A. Foroumadi, A. Shafiee, New tetracyclic tacrine analogs containing pyrano[2,3-c]pyrazole: efficient synthesis, biological assessment and docking simulation study, Eur. J. Med. Chem. 89 (2015) 296–303.

[4] N. Mishra, D. Sasmal, Additional acetyl cholinesterase inhibitory property of diaryl pyrazoline derivatives, Bioorg. Med. Chem. Lett. 23 (3) (2013) 702–705.

[5] M. Atanasova, G. Stavrakov, I. Philipova, D. Zheleva, N. Yordanov, I. Doytchinova, Galantamine derivatives with indole moiety: docking, design, synthesis and acetylcholinesterase inhibitory activity, Bioorg. Med. Chem. 23 (17) (2015) 5382–5389.

[6] C.L. Cardoso, I. Castro-Gamboa, D.H. Silva, M. Furlan, A. Epifanio Rde, C. Pinto Ada, C. Moraes de Rezende, J.A. Lima, S. Bolzani Vda, Indole glucoalkaloids from *Chimarrhis turbinata* and their evaluation as antioxidant agents and acetylcholinesterase inhibitors, J. Nat. Prod. 67 (11) (2004) 1882–1885.

[7] L.C. Klein Jr., C.S. Passos, A.P. Moraes, V.G. Wakui, E.L. Konrath, A. Nurisso, P.A. Carrupt, C.M. de Oliveira, L. Kato, A.T. Henriques, Indole alkaloids and semisynthetic indole derivatives as multifunctional scaffolds aiming the inhibition of enzymes related to neurodegenerative diseases – a focus on *Psychotria* L. Genus, Curr. Top. Med. Chem. 14 (8) (2014) 1056–1075.

[8] C. Sridevi, K. Balaji, A. Naidu, R. Sudhakaran, Antioxidant and antiinflammatory activity of some phenylpyrazolo benzimidazolo quinoxaline derivatives, J. Pharm. Res. 2 (9) (2009) 1370–1372.

[9] A. Aliabadi, A. Foroumadi, A. Mohammadi-Farani, M. Garmsiri Mahvar, Synthesis and evaluation of anti-acetylcholinesterase activity of 2-(2-(4-(2-Oxo-2-phenylethyl)piperazin-1-yl) ethyl)Isoindoline-1,3-dione derivatives with potential anti-alzheimer effects, Iran. J. Basic Med. Sci. 16 (10) (2013) 1049–1054.

[10] N. Khorana, K. Changwichit, K. Ingkaninan, M. Utsintong, Prospective acetylcholinesterase inhibitory activity of indole and its analogs, Bioorg. Med. Chem. Lett. 22 (8) (2012) 2885–2888.

[11] G. Ucar, N. Gokhan, A. Yesilada, A.A. Bilgin, 1-N-Substituted thiocarbamoyl-3-phenyl-5-thienyl-2-pyrazolines: a novel cholinesterase and selective monoamine oxidase B inhibitors for the treatment of Parkinson's and Alzheimer's diseases, Neurosci. Lett. 382 (3) (2005) 327–331.

[12] M. Taha, N.H. Ismail, A. Khan, S.A.A. Shah, A. Anwar, S.A. Halim, M.Q. Fatmi, S. Imran, F. Rahim, K.M. Khan, Synthesis of novel derivatives of oxindole, their urease inhibition and molecular docking studies, Bioorg. Med. Chem. Lett. 25 (16) (2015) 3285–3289.

[13] M. Taha, N.H. Ismail, S. Imran, A. Wadood, F. Rahim, M. Ali, A.U. Rehman, Novel quinoline derivatives as potent *in vitro* [small alpha]-glucosidase inhibitors: in silico studies and SAR predictions, MedChemComm 6 (10) (2015) 1826–1836.

[14] M. Taha, N.H. Ismail, S. Imran, E.H. Anouar, M. Ali, W. Jamil, N. Uddin, S.M. Kashif, Identification of bisindolylmethane-hydrazone hybrids as novel inhibitors of [small beta]-glucuronidase, DFT, and in silico SAR intimations, RSC Adv. 6 (4) (2016) 3276–3289.

[15] M. Taha, N.H. Ismail, S. Imran, M. Selvaraj, F. Rahim, Synthesis of novel inhibitors of [small beta]-glucuronidase based on the benzothiazole skeleton and their molecular docking studies, RSC Adv. 6 (4) (2016) 3003–3012.

[16] N.K. Zawawi, M. Taha, N. Ahmat, A. Wadood, N.H. Ismail, F. Rahim, M. Ali, N. Abdullah, K.M. Khan, Novel 2,5-disubtituted-1,3,4-oxadiazoles with benzimidazole backbone: a new class of beta-glucuronidase inhibitors and in silico studies, Bioorg. Med. Chem. 23 (13) (2015) 3119–3125.

[17] N.K.N.A. Zawawi, M. Taha, N. Ahmat, N.H. Ismail, A. Wadood, F. Rahim, A.U. Rehman, Synthesis, *in vitro* evaluation and molecular docking studies of biscoumarin thiourea as a new inhibitor of α-glucosidases, Bioorg. Chem. 63 (2015) 36–44.

[18] M. Taha, N.H. Ismail, S. Imran, M. Selvaraj, A. Rahim, M. Ali, S. Siddiqui, F. Rahim, K.M. Khan, Synthesis of novel benzohydrazone-oxadiazole hybrids as beta-glucuronidase inhibitors and molecular modeling studies, Bioorg. Med. Chem. 23 (23) (2015) 7394–7404.

[19] G. Brahmachari, C. Choo, P. Ambure, K. Roy, *In vitro* evaluation and *in silico* screening of synthetic acetylcholinesterase inhibitors bearing functionalized piperidine pharmacophores, Bioorg. Med. Chem. 23 (15) (2015) 4567–4575.

[20] A.D.M.E. Rapid, QikProp, Schrödinger LLC, New York, 2012.

[21] R.A. Friesner, J.L. Banks, R.B. Murphy, T.A. Halgren, J.J. Klicic, D.T. Mainz, M.P. Repasky, E.H. Knoll, M. Shelley, J.K. Perry, D.E. Shaw, P. Francis, P.S. Shenkin, Glide: a new approach for rapid, accurate docking and scoring. 1. Method and assessment of docking accuracy, J. Med. Chem. 47 (7) (2004) 1739–1749.

[22] C.A. Lipinski, F. Lombardo, B.W. Dominy, P.J. Feeney, Experimental and computational approaches to estimate solubility and permeability in drug discovery and development settings, Adv. Drug Deliv. Rev. 46 (1–3) (2001) 3–26.

[23] R. Suthakaran, G. Somasekhar, C. Sridevi, M. Marikannan, K. Suganthi, G. Nagarajan, Synthesis, antiinflammatory, antioxidant and antibacterial activities of 7-methoxy benzofuran pyrazoline derivatives, Asian J. Chem. 19 (5) (2007) 3353–3362.

[24] V.H. Babu, C. Sridevi, A. Joseph, K.K. Srinivasan, Synthesis and biological evaluation of some novel pyrazolines, Indian J. Pharm. Sci. 69 (3) (2007) 470–473.

[25] C. Sridevi, K. Balaji, A. Naidu, R. Sudhakaran, Synthesis of some phenylpyrazolo benzimidazolo quinoxaline derivatives as potent antihistaminic agents, E – J. Chem. 7 (1) (2010) 234–238.

[26] A. Voskienė, V. Mickevičius, Cyclization of chalcones to isoxazole and pyrazole derivatives, Chem. Heterocycl. Compd. 45 (12) (2010) 1485–1488.

[27] P. Molyneux, The use of the stable free radical diphenylpicrylhydrazyl (DPPH) for estimating antioxidant activity, Songklanakarin J. Sci. Technol. 26 (2) (2004) 211–219.

[28] M.S. Blois, Antioxidant determinations by the use of a stable free radical, Nature 181 (4617) (1958) 1199–1200.

[29] C. Sridevi, K. Balaji, A. Naidu, R. Sudhakaran, Antioxidant, antiinflammatory and antihistaminic activities of some phenylpyrazolo benzothiazolo quinoxaline derivatives, Int. J. Chem. Sci. 7 (2) (2009) 1117–1126.

[30] R. Re, N. Pellegrini, A. Proteggente, A. Pannala, M. Yang, C. Rice-Evans, Antioxidant activity applying an improved ABTS radical cation decolorization assay, Free Radical Biol. Med. 26 (9–10) (1999) 1231–1237.

[31] G.L. Ellman, K.D. Courtney, V. Andres Jr., R.M. Feather-Stone, A new and rapid colorimetric determination of acetylcholinesterase activity, Biochem. Pharmacol. 7 (1961) 88–95.

[32] G. Kryger, I. Silman, J.L. Sussman, Structure of acetylcholinesterase complexed with E2020 (Aricept): implications for the design of new anti-Alzheimer drugs, Structure (London, England: 1993) 7 (3) (1999) 297–307.

[33] Schrodinger Release 2015-1: Maestro, version 10.1, Schrodinger, LLC, New York, 2015.

[34] PyMOL Molecular Graphics System, Schrodinger LCC., NY, USA, 2010.